Geophysical Research Letters

RESEARCH LETTER
10.1029/2023GL104057

Enhanced Polar Vortex Predictability Following Sudden Stratospheric Warming Events

Philip Rupp[1], Jonas Spaeth[1], Hella Garny[2], and Thomas Birner[1]

[1]Meteorological Institute Munich, Ludwig-Maximilians-University, Munich, Germany, [2]Deutsches Zentrum für Luft- und Raumfahrt (DLR), Institut für Physik der Atmosphäre, Oberpfaffenhofen, Germany

Key Points:

- Sudden stratospheric warmings (SSWs) lead to reduced forecast spread in the polar stratosphere for several weeks after the event
- Reduced forecast spread after SSWs is driven by suppressed vertical planetary wave propagation due to persistent negative wind anomalies
- Final warmings are delayed for winters with SSW, consistent with reduced upward wave fluxes following the SSW

Supporting Information:

Supporting Information may be found in the online version of this article.

Correspondence to:

P. Rupp,
philip.rupp@lmu.de

Citation:

Rupp, P., Spaeth, J., Garny, H., & Birner, T. (2023). Enhanced polar vortex predictability following sudden stratospheric warming events. *Geophysical Research Letters*, *50*, e2023GL104057. https://doi.org/10.1029/2023GL104057

Received 11 APR 2023
Accepted 9 AUG 2023

Abstract Sudden stratospheric warming (SSW) events can form a window of forecast opportunity for polar vortex predictions on subseasonal-to-seasonal time scales. Analyzing numerical ensemble simulations, we quantify the associated enhanced predictability due to reduced upward planetary wave fluxes during the mostly radiatively driven recovery phase following SSWs. Ensembles that predict an SSW show reduced ensemble spread in terms of polar vortex strength for several weeks to follow, as well as a corresponding reduction in forecast errors. This increased predictability is particularly pronounced for strong SSWs and even occurs if not all ensemble members predict a major SSW. Furthermore, we found a direct impact of the occurrence of SSWs on the date of the final warming (FW): the decrease in upward wave fluxes delays the FW significantly. The reduced spread after SSWs and the delay in FW date have potentially further implications for (subseasonal) predictions of the tropospheric and mesospheric circulations.

Plain Language Summary The polar vortex is a large scale circulation active during winter in the higher levels of the polar atmosphere. Changes in the strength of the polar vortex can have an impact on the weather over mid-latitude regions like Europe. This is the case especially for the period after so-called sudden stratospheric warming (SSW) events, where the polar vortex breaks down very abruptly and then slowly recovers over several weeks. Such a break-down of the polar vortex tends to suppress wave activity and hence reduces the dynamical variability in the polar stratosphere, leading to a more predictable evolution of the circulation. We quantify the strength and timescale of this increase in predictability of the polar vortex after an SSW using a large set of winter time model forecasts.

1. Introduction

Among the most extreme dynamical phenomena in Earth's atmosphere are sudden stratospheric warming (SSW) events, with stratospheric polar temperatures increasing by several tens of degrees over the course of a few days. Associated with these warmings is a break-down or even reversal of the westerly zonal mean flow of the stratospheric polar vortex (see review by Baldwin et al. (2021)). Strong disruptions to the stratospheric flow (e.g., around SSWs) tend to last for several weeks and have long been known to affect surface weather (Baldwin & Dunkerton, 2001), with implications for subseasonal-to-seasonal (S2S) forecasts in the troposphere (Baldwin et al., 2003; Kidston et al., 2015; Spaeth & Birner, 2022).

SSW events are predominantly driven by planetary wave activity of tropospheric origin and subsequent wave-mean flow interactions with the polar vortex before and during the event (Matsuno, 1971). The negative wind anomalies formed throughout the SSW, however, tend to suppress subsequent vertical planetary wave propagation (consistent with Charney & Drazin, 1961) and various authors have found a corresponding reduction of upward wave fluxes following the event (Hitchcock et al., 2013; Limpasuvan et al., 2004). Past research has concentrated on the predictability of the tropospheric circulation following SSWs (e.g., Butler et al., 2019a; Domeisen et al., 2020b; Thompson et al., 2002), predicting the SSWs themselves (Chwat et al., 2022; Domeisen et al., 2020a; Stan & Straus, 2009) or predicting the polar vortex strength on seasonal time scales (Maycock et al., 2011; Portal et al., 2022), but the subseasonal predictability of the stratospheric flow following SSWs has not been studied in detail. In the present study we quantify how this reduction in polar stratospheric wave activity after SSWs leads to a significant increase in predictability of the polar vortex strength over the course of several weeks and that SSW events therefore form a window of opportunity for stratospheric forecasts.

Another type of polar vortex breakdowns are so-called final warming (FW) events. They are often conceptually distinguished from mid-winter SSWs, for which the polar vortex needs to recover within the same winter, while

for FWs it does not recover until the following winter (e.g., Charlton & Polvani, 2007). FWs systematically occur in spring time due to the ozone-induced radiative heating over the polar cap, but typically also involve a dynamical component in terms of anomalous upward planetary wave fluxes preceding the event (Black & McDaniel, 2007; Butler et al., 2019b). Given the reduction in upward wave fluxes following SSWs, the question arises whether this impacts the FW date.

The structure of this paper is as follows: Section 2 outlines the data sources used for our analysis and our definition of SSW and FW events. Section 3 presents the obtained results in detail, Section 4 discusses some of the conclusions and Section 5 summarizes our main findings.

2. Data Sources and Event Definition

2.1. Reanalysis

The ERA5 reanalysis data set (Hersbach et al., 2020) of the European Centre for Medium range Weather Forecasts (ECMWF) is used as the representation of atmospheric state and behavior during the winters 1950/51 to 2021/22 and in a climatological sense. It has been shown that incorporating data from the pre-satellite era (before 1979) can enhance studies investigating stratosphere-troposphere coupling, thanks to improved sampling (Hitchcock, 2019). The output is used on a $1° \times 1°$ regular grid following four pressure surfaces (200, 100, 50, and 10 hPa) at a temporal resolution of 6 hr, from which daily averages are computed. The climatological mean has been calculated as inter-annual average of daily values and was smoothed using a centered 30 days running mean to reduce high frequency variability. Throughout the manuscript we interpret diagnostics based on reanalysis data as observations and thus the true state of the atmosphere.

2.2. Model Forecasts

The S2S prediction project (Vitart et al., 2017) provides a collection of extended-range ensemble forecasts from different weather services. For the purpose of this study we use the S2S ensemble forecasts generated by ECMWF, which cover leadtimes up to 46 days. Post-processed output analyzed in this study is given in the form of 24-hourly instantaneous fields at $2.5° \times 2.5°$ horizontal resolution and on four pressure levels (200, 100, 50, and 10 hPa). These forecasts are initialized twice a week and we analyze real-time winter forecasts (16 November to 22 February) initialized between late 2017 and early 2021, for which the model versions only vary marginally. Besides the 51-member real-time forecasts, each initialization includes a set of 11-member hindcasts, initialized with initial and boundary conditions covering the same date for the 20 years prior to the respective real-time simulation. These hindcasts are used to construct a climatology and calculate corresponding anomalies. The climatological mean for a given forecast-day is calculated leadtime dependent as average over all hindcast members of ensembles initialized within a ± 15 days window around the initialization date of the respective forecast. It is further smoothed with a 7-day running mean. Overall, our analyses include 114 real-time forecast ensembles and 2,280 hindcasts resulting in a total of 30,894 individual model runs. More details on the S2S data set used here can be found in Spaeth and Birner (2022).

2.3. Specification of Sudden Stratospheric Warming and Final Warming Events

We identify SSW events that occurred in the real atmosphere using the criterion from Charlton and Polvani (2007), who specify the SSW onset day via the reversal of the zonal mean zonal wind at 60°N and 10 hPa (U^{10}_{60}, a measure for the polar vortex strength). This way we identify 48 SSW events within the period of available ERA5 data (1950–2022). The retrieved SSW dates are almost identical to the ones identified by Butler et al. (2017) within the overlapping time period; minor differences could arise from the use of a different data set. Note that we find 39 winter periods with an SSW, of which nine winters experience two SSWs. This gives an average frequency of about 0.67 SSWs/winter, although only about 54% of the winters experience an SSW. Within the period of available S2S forecasts (1997–2021) we identify 15 observed SSWs.

We then select a total of 100 ensemble forecasts that were initialized within ± 3 days of these 15 observed SSWs (hereafter referred to as "SSW initializations"). These consist of 94 hindcasts of 11 members and 6 real-time forecasts of 51 members (1,340 individual runs). We furthermore classify the observed SSWs in terms of their strength, where strong, moderate and weak SSWs are defined as lower, middle and upper third of U^{10}_{60} averaged

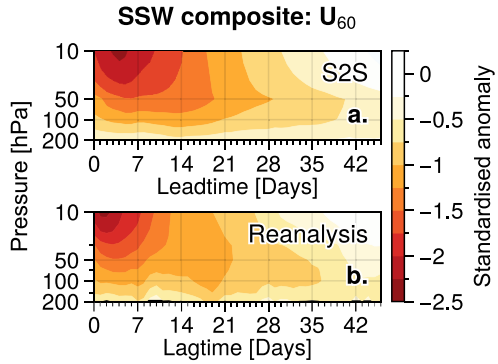

Figure 1. (a) Composite mean evolution of standardized zonal mean zonal wind at 60°N (U_{60}) on different pressure levels averaged over 100 sudden stratospheric warming (SSW) forecasts (i.e., ensembles initialized within ±3 days relative to one of 15 observed SSWs) as a function of leadtime relative to the initialization date. (b) composite mean evolution in reanalysis data as a function of lag relative to the 48 SSWs observed in the period of available re-analysis data.

over lags +7 to +13 relative to the onset date. This leads to 68 strong/medium SSW forecasts and 32 weak SSW forecasts. A group of "climatological initializations" is given by all 2,394 available forecast ensembles. Lists of identified events and utilized S2S forecasts within the SSW initialization group are provided in Supporting Information S1 as Tables S1 and S2.

Figure 1 compares the composite mean evolution of the standardised stratospheric zonal mean zonal winds at 60°N (U_{60}) in S2S forecasts and reanalysis data following observed SSWs. Both data sets show a pronounced negative wind anomaly reaching two standard deviations and persisting for about 6 weeks in the lower/middle stratosphere. The good agreement between the two data sources in terms of composite mean evolution gives confidence in an adequate representation of SSWs within the model forecasts. Note that the larger ensemble size of the S2S composite compared to ERA5 leads to a generally smoother evolution of the composite mean.

We further identify FW events as the first day of negative U_{60}^{10} within a calendar year that is preceded by positive winds and is not followed by more than 10 days of positive wind before the end of May (consistent with Butler & Domeisen, 2021; Charlton & Polvani, 2007). This criterion defines precisely one FW event per winter season.

3. Results

Figure 2a shows the composite evolution of polar vortex variability in terms of the square root of the averaged ensemble variance (from now on referred to as ensemble spread) in S2S forecasts of the zonal mean zonal wind at 60°N and 10 hPa (U_{60}^{10}) for ensembles either initialized around onset dates of observed SSWs or for all available initializations (climatology). The initial evolution of ensemble spread is dominated by exponential growth irrespective of whether an SSW happened around the initialization or not. However, from about day 14 onwards the spread evolutions of climatological and SSW initializations start to diverge. While the climatological spread reaches values of roughly 14 m/s toward the end of the simulation (about 40 days), the spread of SSW initializations already converges after about 3 weeks near 8 m/s (roughly half of the climatological spread).

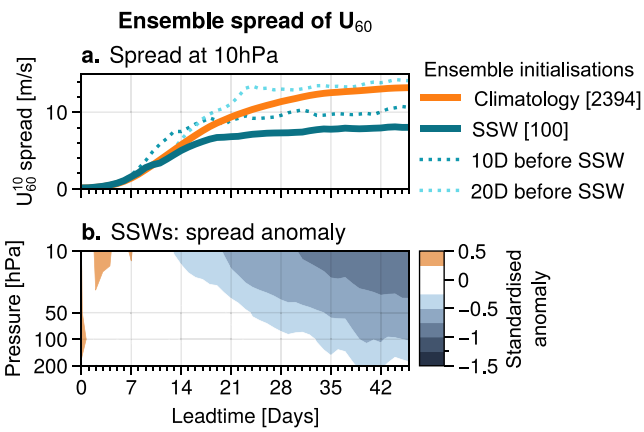

Figure 2. (a) Evolution of U_{60}^{10} ensemble spread in terms of square root of the average ensemble variance over all forecast initializations (climatology) and over sudden stratospheric warming (SSW) initializations. Dotted lines show the spread evolution of forecasts initialized 10 or 20 days ahead of an SSW. Numbers in square brackets indicate the number of ensemble forecasts within the respective group. (b) Standardized (w.r.t. the leadtime, season and model-version dependent, climatological distribution of ensemble spread) anomaly of the U_{60} ensemble spread within SSW forecast initializations compared to climatological initializations. All shown anomalies are significant ($p < 0.05$).

We further find that the final ensemble spread at several weeks leadtime is still substantially reduced if the forecast is initialized several days before an SSW (but still within the predictability window of the event). Only if initialized at least about 3 weeks prior to the event (when essentially all predictability of the SSW itself is lost) does the spread evolution reach climatological values at the end of the simulation. In general the post-SSW evolution is very robust in terms of ensemble spread and mean (not shown) for strong and medium SSWs (see Section 2.3) even when initialized with a lag of about ±2 weeks around the event onset date, while weak SSWs show very limited systematic behavior.

Figure 2b shows that the standardized negative ensemble spread anomalies of U_{60}^{10} in SSW initializations are persistently around one standard deviation at 10 hPa from about week 4 onwards and span the entire middle and lower stratosphere after about 5 weeks. A reduction in ensemble spread can be interpreted as an increase in confidence of the numerical model regarding its prediction. In order to analyze if this increase in confidence also corresponds to an actual improvement of the model forecasts (i.e., an increase in predictability) we analyze the model skill in terms of absolute forecast errors of the U_{60} index. Figure 3a shows a gradual increase in error throughout the simulation for climatological initializations. However, the mean error is substantially reduced (up to about 60%) for forecasts initialized around an SSW

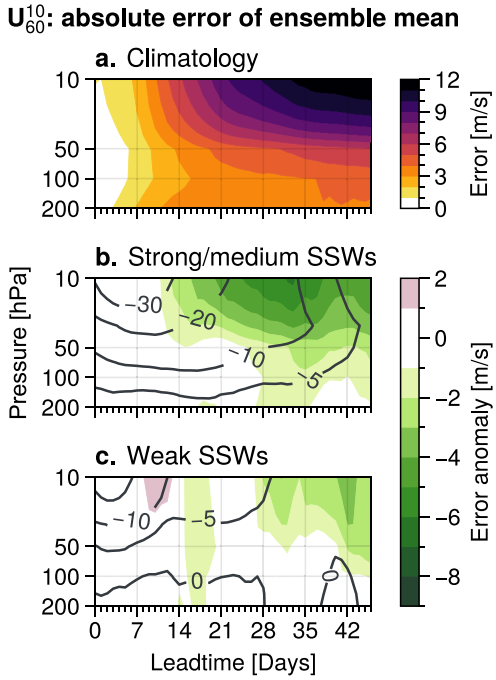

Figure 3. (a) Absolute error of the ensemble mean of U_{60} anomalies w.r.t. reanalysis evolution averaged over all forecasts (climatology). (b, c) The average anomaly of the absolute error for Sudden stratospheric warming (SSW) initializations corresponding to strong/medium and weak SSWs (see Section 2.3), respectively. Contour lines show composite mean U_{60} anomalies (in m/s).

event (Figure 3b). This increase in predictability is particularly pronounced at 10 hPa after about week 5 and for forecasts initialized around strong and medium SSWs (events sufficiently negative mean U_{60}^{10} during second week after the event). SSW events associated with weak or non-persistent stratospheric zonal mean wind anomalies do only have a minor effect on the forecast errors (Figure 3c). Note that using different metrics to assess the model skill (e.g., root mean squared error - RMSE) gives qualitatively very similar results (not shown).

Figure 4 shows that persistently strong negative wind anomalies formed during the SSW subsequently suppress the vertical propagation of planetary waves into the stratosphere, which ultimately acts to increase stratospheric predictability following SSWs. Consequently, Figure 4a shows a significant positive correlation of stratospheric wind anomalies (polar vortex strength) and lower stratospheric heat flux anomalies, as shown by a pronounced separation of SSW and climatological ensemble initializations. While the climatological forecast distribution is necessarily distributed around zero anomalies, SSW initializations are clearly associated with negative heat flux anomalies and negative polar vortex strengths (the latter by construction). This effect is particularly pronounced for strong and medium SSWs, while for weak SSWs the values lie well within climatological variability. The reduction in stratospheric wave activity due to the weakened heat flux after SSWs, in turn, substantially reduces the amount of dynamic variability of the polar vortex and hence reduces the growth of ensemble spread in polar vortex strength predictions (Figure 4b).

Figure 4c shows a direct correlation between the negative stratospheric zonal wind anomalies created during the SSW and the reduced spread at the end of ensemble simulations initialized around the SSW onset. When considering all SSWs (strong, medium, and weak events), we find a corresponding correlation within the individual cluster of SSW initializations itself (correlation coefficient $r = 0.33$, $p < 0.001$). However, this correlation mostly results from a few outliers associated with weak SSWs, which formally satisfy the definition of an SSW, but do not create sufficiently persistent and strong negative stratospheric wind anomalies to substantially reduce upward planetary wave propagation. These weak SSWs therefore have a limited dynamical effect on the subsequent polar vortex evolution and the corresponding ensembles behave more like ensembles not associated with an SSW (this is also consistent with Figure 3c). The correlation of polar vortex

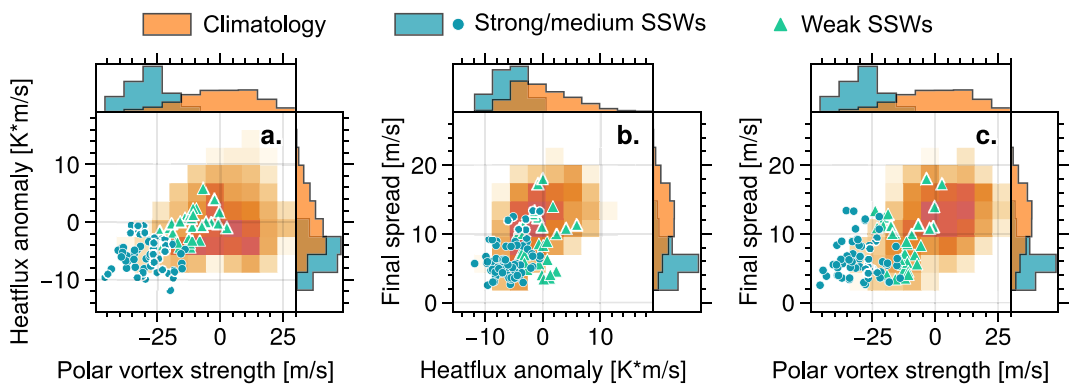

Figure 4. Scatter plots of different metrics calculated from all forecast initializations (climatology) and sudden stratospheric warming (SSW) ensemble initializations. Metrics are polar vortex strength (U_{60}^{10} anomaly averaged over days +7 to +13), heat flux anomaly (wave number 1 eddy heat flux at 100 hPa averaged over days +14 to +34) and final spread (square root of the mean ensemble variance of U_{60}^{10} averaged over days +35 to +41). SSW initializations are divided into strong/medium and weak cases (see Section 2.3). The shading denotes the bivariate distributions derived from all available forecasts. Histograms show univariate and normalized distributions for the climatological and strong/medium SSW initializations.

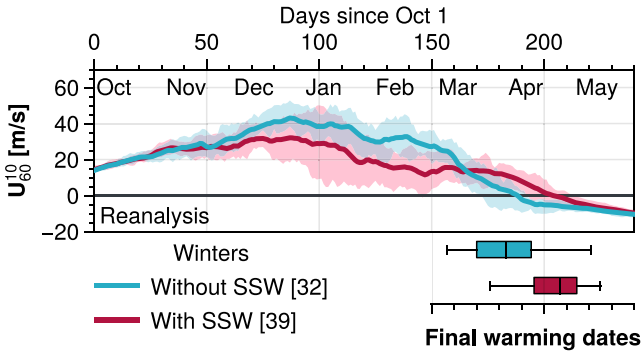

Figure 5. Climatological evolution of U_{60}^{10} in reanalysis data. Years are averaged separately for winters with and without sudden stratospheric warming; numbers in brackets denote cluster sizes. Solid lines show the mean and shading shows inner-quartiles. Box plots indicate the distributions in final warming dates for the two clusters, with black lines giving the median, box-edges the inner-quartiles and whiskers the minima and maxima.

strength and final spread vanished when considering strong/medium SSW initializations only ($r = 0.02$). Note that we find a significant correlation within the climatological cluster with all initializations ($r = 0.39$, $p < 0.001$), presumably due to the fact that the climatology contains a substantial number of ensembles which are initialized a certain time before or after the SSW (Figure 2 shows that the spread is reduced even if the ensemble is initialized 10 days before the SSW and that the spread reduction lasts for several weeks afterward).

The results shown in Figure 4c suggest that SSWs may be thought of as triggering a regime transition of the stratospheric circulation. The system either enters a state with persistently strong negative anomalies in stratospheric zonal winds and planetary wave activity (leading to increased predictability) or more rapidly returns to a robust polar vortex that supports planetary wave propagation (leading to almost climatological behavior). Each of these two forecast clusters (SSWs and climatological states) show relatively small case-to-case variability and no substantial correlation between polar vortex strength and upward wave propagation. Common criteria to define SSWs based solely on the instantaneous reversals of the flow and not considering the formation of persistent wind anomalies or their effect on wave activity may struggle to distinguish between these cases. Further note that the predictability of SSWs themselves can depend on various factors, including metrics that might correlate with the SSW strength (e.g., Chwat et al., 2022; Wu et al., 2022).

The suppression of vertical planetary wave propagation for several weeks following SSWs suggests a robust delay of FW dates in winters with an SSW compared to winters without, and this is indeed the case (Figure 5). Specifically, we find an anomalously strong polar vortex during April for winters with SSWs, even though the vortex is anomalously weak during December–February in those winters (by construction due to the occurrence of SSWs). This relative strengthening is also consistent with a less perturbed radiative recovery of the vortex following the sudden warming (e.g., Bloxam & Huang, 2021). On average, polar stratospheric westerlies are sustained through mid April in winters with SSWs, hence about 3 weeks longer than in winters without SSW, leading to a robust shift of the FW date distribution. Since FW events are to some extent dynamically driven (i.e., preceded by increased upward flux of planetary waves), a corresponding delay of the FW is consistent with the reduction of upward wave fluxes following the SSW (cf. Figure 4a). Note that most winters with SSW occurring early in the season (November or December) also experience a second SSW later-on (5 out of 7).

4. Discussion

The predictability of the polar vortex increases substantially due to reduced upward wave fluxes following SSWs, leading to potential implications for the predictability of tropospheric and upper-atmospheric circulation, which should be investigated in detail in future studies. For example, the role of SSWs for providing predictive skill in the mesosphere and upper atmosphere is increasingly being appreciated (e.g., Pedatella et al., 2018; Sassi et al., 2019). In particular, the wind reversal during SSWs acts as filter for gravity waves, which are of major importance for driving middle and upper atmospheric flows and determining the variability in those layers. Longer predictive skill in the stratosphere after strong SSWs should therefore also provide a window of forecast opportunity for the upper atmosphere—a topic also relevant for space technology (e.g., Pedatella et al., 2018).

Furthermore, the details of when and how the FW occurs might have implications for the predictability of the tropospheric and mesospheric circulation (e.g., Hardiman et al., 2011). Studies have found robust tropospheric (Black et al., 2006; Sun & Robinson, 2009) and mesospheric (Pancheva et al., 2009; Yamazaki & Matthias, 2019) flow anomalies following FWs. Due to the delay of the FW in years with SSW we can expect a corresponding delay of the associated tropospheric and mesospheric signatures in those years.

5. Summary and Conclusions

We have quantified the reduction in ensemble spread in stratospheric polar vortex strength at subseasonal time scales for forecasts initialized around the onset of a SSW event. This reduction is due to the well-known

suppression of upward planetary wave propagation in the stratosphere and the associated suppression of stratospheric dynamical variability. Our results show the effect to be robust for strong SSWs and present even if the forecast is initialized several days before the event. The reduced ensemble spread is linked to a notable decrease in stratospheric forecast errors for a period of several weeks. Hence, SSW events can be considered as a window of forecast opportunity for the polar stratospheric flow well beyond the SSW event itself. Furthermore, the decrease in upward wave fluxes following SSWs is consistent with a delay of the FW by about 3 weeks in winters with SSW, compared to winters without. The established upward and downward coupling following SSWs and FWs suggests important associated implications for the predictability of tropospheric and mesospheric circulations.

Data Availability Statement

The ERA5 re-analysis and S2S forecast data sets used in this study can be accessed via the ECMWF website (ECMWF, 2015, 2018). Details on the specifics of the data sets and how they were processed are provided in Section 2. Lists of the identified events and utilized forecast ensembles are provided in the Supporting Information S1, as well as the following repository: https://doi.org/10.5282/ubm/data.395.

Acknowledgments
This research has been supported by the Deutsche Forschungsgemeinschaft (DFG; Grant SFB/TRR165, "Waves to Weather"). We want to thank two anonymous referees for their extensive comments that helped to improve this manuscript. Open Access funding enabled and organized by Projekt DEAL.

References

Baldwin, M. P., Ayarzagüena, B., Birner, T., Butchart, N., Butler, A. H., Charlton-Perez, A. J., et al. (2021). Sudden stratospheric warmings. *Reviews of Geophysics*, *59*(1), e2020RG000708. https://doi.org/10.1029/2020rg000708

Baldwin, M. P., & Dunkerton, T. J. (2001). Stratospheric harbingers of anomalous weather regimes. *Science*, *294*(5542), 581–584. https://doi.org/10.1126/science.1063315

Baldwin, M. P., Stephenson, D. B., Thompson, D. W., Dunkerton, T. J., Charlton, A. J., & O'Neill, A. (2003). Stratospheric memory and skill of extended-range weather forecasts. *Science*, *301*(5633), 636–640. https://doi.org/10.1126/science.1087143

Black, R. X., & McDaniel, B. A. (2007). The dynamics of northern hemisphere stratospheric final warming events. *Journal of the Atmospheric Sciences*, *64*(8), 2932–2946. https://doi.org/10.1175/jas3981.1

Black, R. X., McDaniel, B. A., & Robinson, W. A. (2006). Stratosphere–troposphere coupling during spring onset. *Journal of Climate*, *19*(19), 4891–4901. https://doi.org/10.1175/jcli3907.1

Bloxam, K., & Huang, Y. (2021). Radiative relaxation time scales quantified from sudden stratospheric warmings. *Journal of the Atmospheric Sciences*, *78*(1), 269–286. https://doi.org/10.1175/jas-d-20-0015.1

Butler, A. H., Charlton-Perez, A., Domeisen, D. I., Garfinkel, C., Gerber, E. P., Hitchcock, P., et al. (2019a). Chapter 11—Sub-seasonal predictability and the stratosphere. In A. W. Robertson & F. Vitart (Eds.), *Sub-seasonal to seasonal prediction* (pp. 223–241). Elsevier. Retrieved from https://www.sciencedirect.com/science/article/pii/B9780128117149000115

Butler, A. H., Charlton-Perez, A., Domeisen, D. I., Simpson, I. R., & Sjoberg, J. (2019b). Predictability of northern hemisphere final stratospheric warmings and their surface impacts. *Geophysical Research Letters*, *46*(17–18), 10578–10588. https://doi.org/10.1029/2019gl083346

Butler, A. H., & Domeisen, D. I. (2021). The wave geometry of final stratospheric warming events. *Weather and Climate Dynamics*, *2*(2), 453–474. https://doi.org/10.5194/wcd-2-453-2021

Butler, A. H., Sjoberg, J. P., Seidel, D. J., & Rosenlof, K. H. (2017). A sudden stratospheric warming compendium. *Earth System Science Data*, *9*(1), 63–76. https://doi.org/10.5194/essd-9-63-2017

Charlton, A. J., & Polvani, L. M. (2007). A new look at stratospheric sudden warmings. Part I: Climatology and modeling benchmarks. *Journal of Climate*, *20*(3), 449–469. https://doi.org/10.1175/jcli3996.1

Charney, J., & Drazin, P. (1961). Propagation of planetary scale waves from the lower atmosphere to the upper atmosphere. *Journal of Geophysical Research*, *66*(1), 83–109. https://doi.org/10.1029/jz066i001p00083

Chwat, D., Garfinkel, C. I., Chen, W., & Rao, J. (2022). Which sudden stratospheric warming events are most predictable? *Journal of Geophysical Research: Atmospheres*, *127*(18), e2022JD037521. https://doi.org/10.1029/2022jd037521

Domeisen, D. I., Butler, A. H., Charlton-Perez, A. J., Ayarzagüena, B., Baldwin, M. P., Dunn-Sigouin, E., et al. (2020a). The role of the stratosphere in subseasonal to seasonal prediction: 1. Predictability of the stratosphere. *Journal of Geophysical Research: Atmospheres*, *125*(2), e2019JD030920. https://doi.org/10.1029/2019JD030920

Domeisen, D. I., Butler, A. H., Charlton-Perez, A. J., Ayarzagüena, B., Baldwin, M. P., Dunn-Sigouin, E., et al. (2020b). The role of the stratosphere in subseasonal to seasonal prediction: 2. Predictability arising from stratosphere-troposphere coupling. *Journal of Geophysical Research: Atmospheres*, *125*(2), e2019JD030923. https://doi.org/10.1029/2019jd030923

ECMWF. (2015). S2S forecast database. https://apps.ecmwf.int/datasets/data/s2s-realtime-instantaneous-accum-ecmf/levtype=sfc/type=cf/

ECMWF. (2018). ERA-5 re-analysis. https://cds.climate.copernicus.eu/cdsapp#!/dataset/reanalysis-era5-pressure-levels?tab=overview

Hardiman, S. C., Butchart, N., Charlton-Perez, A. J., Shaw, T. A., Akiyoshi, H., Baumgaertner, A., et al. (2011). Improved predictability of the troposphere using stratospheric final warmings. *Journal of Geophysical Research*, *116*(D18), D18113. https://doi.org/10.1029/2011jd015914

Hersbach, H., Bell, B., Berrisford, P., Hirahara, S., Horányi, A., Muñoz-Sabater, J., et al. (2020). The ERA5 global reanalysis. *Quarterly Journal of the Royal Meteorological Society*, *146*(730), 1999–2049. https://doi.org/10.1002/qj.3803

Hitchcock, P. (2019). On the value of reanalyses prior to 1979 for dynamical studies of stratosphere–troposphere coupling. *Atmospheric Chemistry and Physics*, *19*(5), 2749–2764. https://doi.org/10.5194/acp-19-2749-2019

Hitchcock, P., Shepherd, T. G., & Manney, G. L. (2013). Statistical characterization of arctic polar-night jet oscillation events. *Journal of Climate*, *26*(6), 2096–2116. https://doi.org/10.1175/jcli-d-12-00202.1

Kidston, J., Scaife, A. A., Hardiman, S. C., Mitchell, D. M., Butchart, N., Baldwin, M. P., & Gray, L. J. (2015). Stratospheric influence on tropospheric jet streams, storm tracks and surface weather. *Nature Geoscience*, *8*(6), 433–440. https://doi.org/10.1038/ngeo2424

Limpasuvan, V., Thompson, D. W., & Hartmann, D. L. (2004). The life cycle of the northern hemisphere sudden stratospheric warmings. *Journal of Climate*, *17*(13), 2584–2596. https://doi.org/10.1175/1520-0442(2004)017<2584:tlcotn>2.0.co;2

Matsuno, T. (1971). A dynamical model of the stratospheric sudden warming. *Journal of the Atmospheric Sciences*, *28*(8), 1479–1494. https://doi.org/10.1175/1520-0469(1971)028<1479:admots>2.0.co;2

Maycock, A. C., Keeley, S. P., Charlton-Perez, A. J., & Doblas-Reyes, F. J. (2011). Stratospheric circulation in seasonal forecasting models: Implications for seasonal prediction. *Climate Dynamics*, *36*(1–2), 309–321. https://doi.org/10.1007/s00382-009-0665-x

Pancheva, D., Mukhtarov, P., Andonov, B., Mitchell, N. J., & Forbes, J. (2009). Planetary waves observed by timed/saber in coupling the stratosphere–mesosphere–lower thermosphere during the winter of 2003/2004: Part 1—Comparison with the UKMO temperature results. *Journal of Atmospheric and Solar-Terrestrial Physics*, *71*(1), 61–74. https://doi.org/10.1016/j.jastp.2008.09.016

Pedatella, N., Chau, J., Schmidt, H., Goncharenko, L., Stolle, C., Hocke, K., et al. (2018). How sudden stratospheric warmings affect the whole atmosphere.

Portal, A., Ruggieri, P., Palmeiro, F. M., García-Serrano, J., Domeisen, D. I., & Gualdi, S. (2022). Seasonal prediction of the boreal winter stratosphere. *Climate Dynamics*, *58*(7–8), 2109–2130. https://doi.org/10.1007/s00382-021-05787-9

Sassi, F., McCormack, J., & McDonald, S. (2019). Whole atmosphere coupling on intraseasonal and interseasonal time scales: A potential source of increased predictive capability. *Radio Science*, *54*(11), 913–933. https://doi.org/10.1029/2019rs006847

Spaeth, J., & Birner, T. (2022). Stratospheric modulation of arctic oscillation extremes as represented by extended-range ensemble forecasts. *Weather and Climate Dynamics*, *3*(3), 883–903. https://doi.org/10.5194/wcd-3-883-2022

Stan, C., & Straus, D. M. (2009). Stratospheric predictability and sudden stratospheric warming events. *Journal of Geophysical Research*, *114*(D12), D12103. https://doi.org/10.1029/2008jd011277

Sun, L., & Robinson, W. A. (2009). Downward influence of stratospheric final warming events in an idealized model. *Geophysical Research Letters*, *36*(3), L03819. https://doi.org/10.1029/2008gl036624

Thompson, D. W., Baldwin, M. P., & Wallace, J. M. (2002). Stratospheric connection to northern hemisphere wintertime weather: Implications for prediction. *Journal of Climate*, *15*(12), 1421–1428. https://doi.org/10.1175/1520-0442(2002)015<1421:sctnhw>2.0.co;2

Vitart, F., Ardilouze, C., Bonet, A., Brookshaw, A., Chen, M., Codorean, C., et al. (2017). The subseasonal to seasonal (S2S) prediction project database. *Bulletin of the American Meteorological Society*, *98*(1), 163–173. https://doi.org/10.1175/bams-d-16-0017.1

Wu, R. W.-Y., Wu, Z., & Domeisen, D. I. (2022). Differences in the sub-seasonal predictability of extreme stratospheric events. *Weather and Climate Dynamics*, *3*(3), 755–776. https://doi.org/10.5194/wcd-3-755-2022

Yamazaki, Y., & Matthias, V. (2019). Large-amplitude quasi-10-day waves in the middle atmosphere during final warmings. *Journal of Geophysical Research: Atmospheres*, *124*(17–18), 9874–9892. https://doi.org/10.1029/2019jd030634